Supporting Information: Area-Type Electronic Bipolar Switching Al/TiO$_{1.7}$/TiO$_2$/Al Memory with Linear Potentiating and Depressing Characteristics

Yu Yan, [1] *Jia Cheng Li,* [1] *Yu Ting Chen,* [1] *Xiang Yu Wang,* [1] *Gang Ri Cai,* [2] *Hyeon Woo Park,* [3] *Ji Hun Kim,* [3] *Jin Shi Zhao*,* [1] *and Cheol Seong Hwang*,* [3]

[1] Tianjin Key Laboratory of Film Electronic & Communication Devices, School of Integrated Circuit Science and Engineering, Tianjin University of Technology, No. 391, Binshuixi Road, Xiqing District, Tianjin, 300384, China.

[2] Tianjin Key Laboratory of Organic Solar Cells and Photochemical Conversion, School of Chemistry and Chemical Engineering, Tianjin University of Technology, No. 391, Binshuixi Road, Xiqing District, Tianjin, 300384, China.

[3] Department of Materials Science and Engineering and Inter-university Semiconductor Research Center, Seoul National University, Gwanak-ro 1, Daehag-dong, Gwanak-gu, Seoul, 08826, Republic of Korea.

* Corresponding author's email address: jinshi58@163.com (Jin Shi Zhao) and cheolsh@snu.ac.kr (Cheol Seong Hwang)
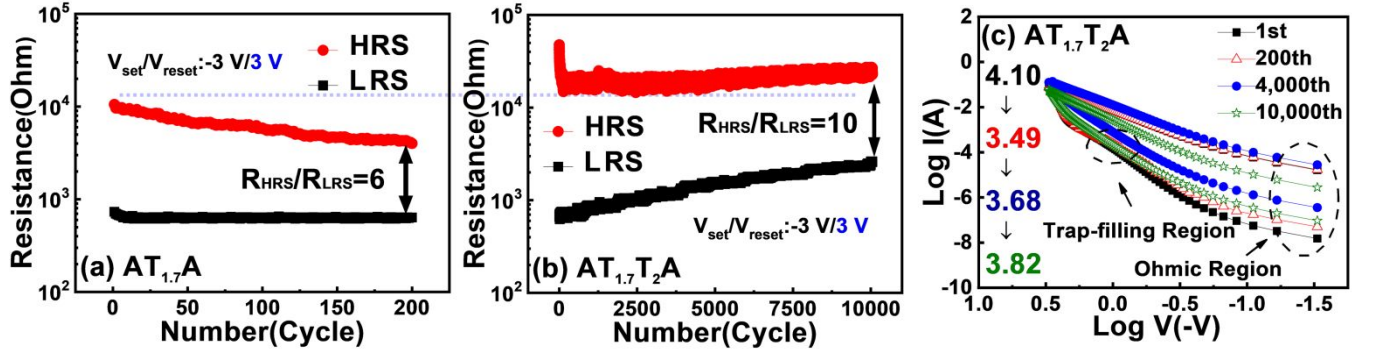
Figure S1. Endurance performance with V_{set}@-3 V and V_{reset}@3 V of the (a) $AT_{1.7}A$ and (b) $AT_{1.7}T_2A$ devices under I-V sweep. (c) SCLC fitting results from the double-log scale for different repetition cycles of the $AT_{1.7}T_2A$ device.
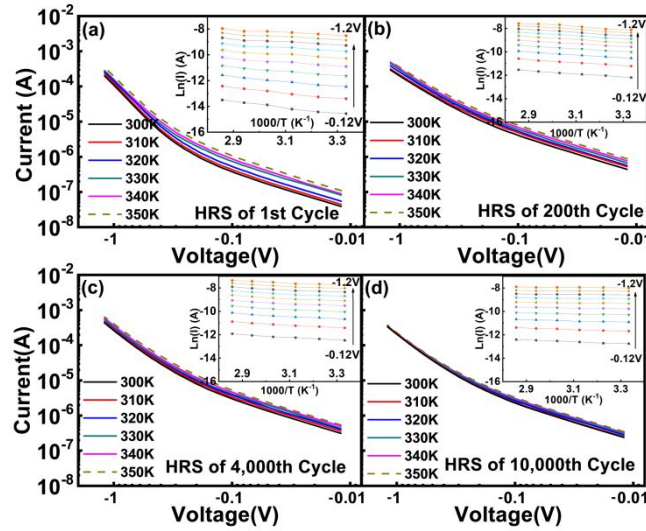

Figure S2. Electrical conduction behaviors in the narrow voltage bias region measured from 300K to 350 K. HRS of the sample after (a) the first, (b) 200th, (c) 4,000th, and (d) 10,000th I-V sweep. The inset figure shows the Arrhenius-type plots in the corresponding I-V curves, from which the activation energy (E_a)
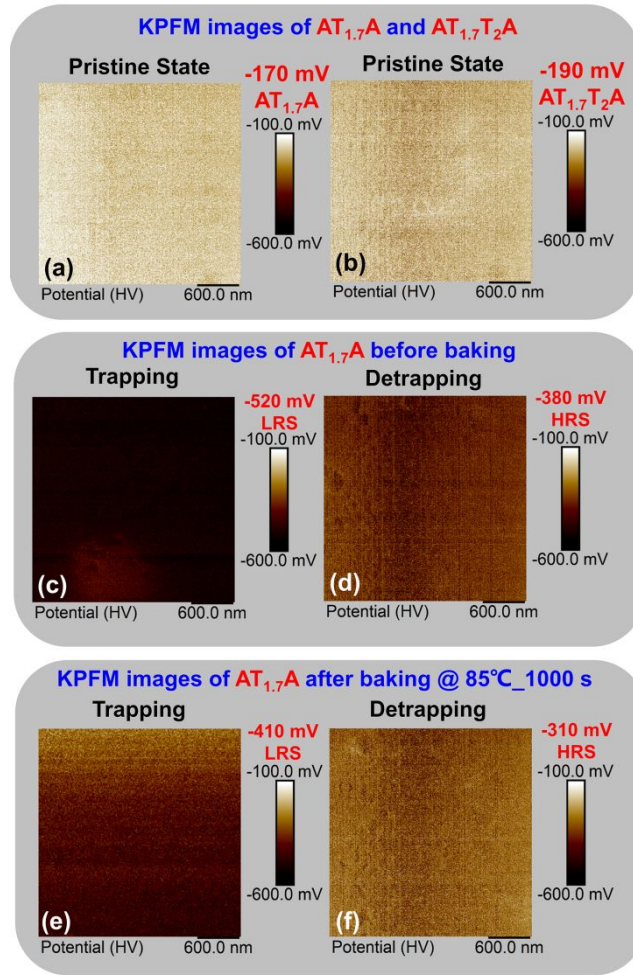
could be estimated as a function of the applied voltage.
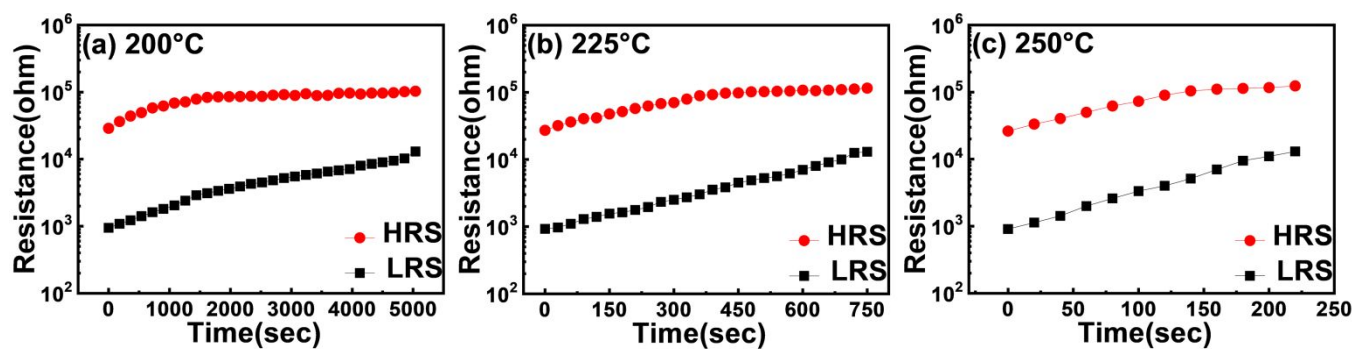


Figure S3. Retention test of the $AT_{1.7}T_2A$ sample performed at (a) 200℃, (b) 225℃, and (c) 250℃, respectively.
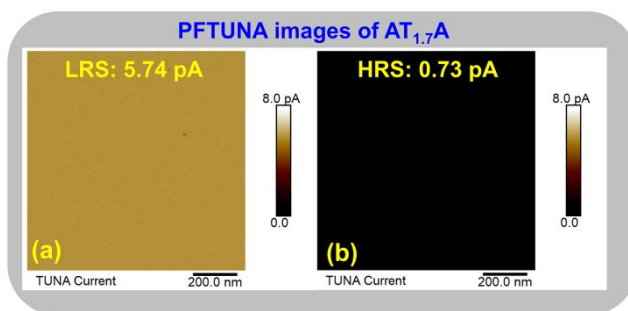

Figure S4. PFTUNA images of the $AT_{1.7}A$ devices of (a) LRS before baking and (b) HRS before baking.

KPFM images of AT$_{1.7}$A and AT$_{1.7}$T$_2$A

Pristine State — -170 mV AT$_{1.7}$A

Pristine State — -190 mV AT$_{1.7}$T$_2$A

(a) Potential (HV) 600.0 nm

(b) Potential (HV) 600.0 nm

KPFM images of AT$_{1.7}$A before baking

Trapping — -520 mV LRS

Detrapping — -380 mV HRS

(c) Potential (HV) 600.0 nm

(d) Potential (HV) 600.0 nm

KPFM images of AT$_{1.7}$A after baking @ 85℃_1000 s

Trapping — -410 mV LRS

Detrapping — -310 mV HRS

(e) Potential (HV) 600.0 nm

(f) Potential (HV) 600.0 nm

Figure S5. KPFM surface potential distribution images of the pristine states of the (a) AT$_{1.7}$A and (b) AT$_{1.7}$T$_2$A devices. KPFM results of the (c) electron-trapped (LRS) and (d) detrapped (HRS) states of the AT$_{1.7}$A structure. KPFM results of the (e) electron-trapped (LRS) and (f) detrapped (HRS) states of the AT$_{1.7}$A structure after baking for 1,000 s at 85℃.
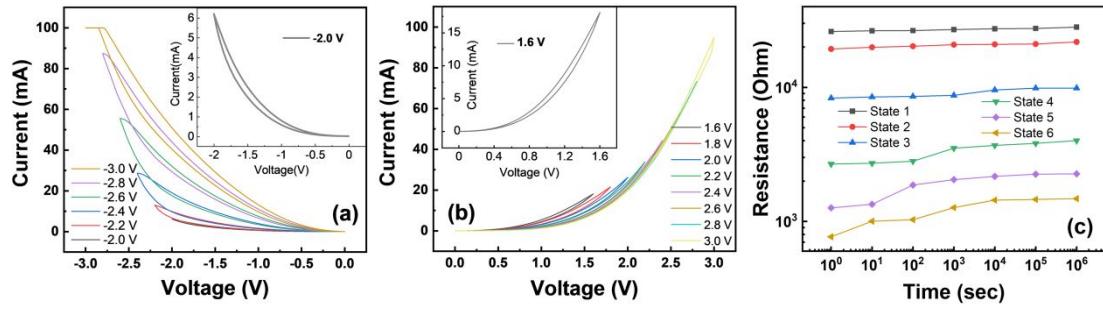
Figure S6. Multi-level current values of the $AT_{1.7}T_2A$ structure (a) using the negative sweep mode for potentiation with an increasing (absolutely increasing) stop voltage (inset: -2 V stop voltage), (b) using the positive sweep mode for depression with an increasing stop voltage (inset: 1.6 V stop voltage) and (c) the retention of the multi-level states (read voltage was -0.1 V) achieved in (a) at room temperature.
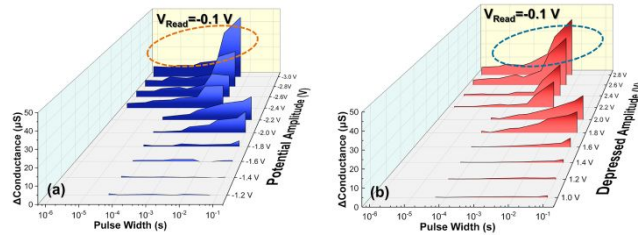
Figure S7. Measured conductance changes of the $AT_{1.7}T_2A$ structure after application of different voltage pulse widths and voltage amplitudes. (a) Potentiation. (b) Depression.